A PARAMETERISATION OF SHALLOW CUMULUS CONVECTION

M.J. Manton*
European Centre for Medium Range Weather Forecasts
Reading, U.K.

A convection scheme is developed for shallow cumulus clouds which are supported by thermals driven by the surface fluxes of heat and moisture. By penetrating the stable region above the mixed layer, the clouds enhance the turbulent mixing in the boundary layer. This effect is modelled by adjusting the turbulent eddy diffusivity in the region below cloud top. The convection scheme provides an estimate of the fractional cloud cover due to shallow cumulus and so it could be used in conjunction with the computation of radiative transfer in the boundary layer.

*Visiting Scientist from CSIRO, Australia

1. INTRODUCTION

Analysis of the predictions of the ECMWF forecast model (Tiedtke, 1981) shows that vertical diffusion is represented reasonably well in most areas of the world. However, it is apparent that the ECMWF model underestimates the vertical transport of moisture from the tropical oceans into the troposphere. Such transport is supported in the atmosphere by shallow cumulus clouds that penetrate the trade-wind inversion.

Cumulus convection in the ECMWF large-scale model is represented currently by the Kuo (1974) scheme. The Kuo scheme assumes that cumulus clouds form when the convergence of moisture (represented by the rate of change of humidity) is appropriately high and the surface air is conditionally unstable. It is found within the ECMWF forecast model that Kuo-type clouds are suppressed by a strong trade-wind inversion. Consequently moisture is trapped in the well-mixed layer where it may be removed by large-scale condensation. Thus the mixed layer is found to be unrealistically shallow and the flux of moisture into the middle troposphere is underestimated.

In the present work we describe a cumulus convection scheme in which cloud is assumed to form above the well-mixed layer if thermals originating from the surface layer are sufficiently intense. The main effect of the clouds is to enhance the turbulent mixing in the stable region above the mixed layer. Thus the eddy diffusivity is appropriately adjusted to account for the increased turbulence below cloud top. By comparing the distance that thermals penetrate into the inversion with the condensation level of the thermal, an estimate of the cloud cover is obtained. The present convection scheme therefore could be used to provide the interaction between radiative transfer and turbulent mixing that occurs in regions of shallow cumulus convection.

2. EFFECT OF CLOUD ON MIXING

When turbulent mixing is parameterized by an eddy diffusivity K_Q, the buoyancy flux in the absence of condensation is represented by

$$g\,\overline{\rho' w'}/\rho = K_Q B, \tag{2.1}$$

where $B = g\left\{\frac{1}{\theta}\frac{\partial\theta}{\partial z} + (R_v/R_a\ 1)\frac{\partial q}{\partial z}\right\}$,

Rv and Ra are the gas constants for water vapour and dry air, g is the gravitational acceleration, ρ is the air density, w is the vertical velocity, θ is the potential temperature, q is the total mass fraction of water and z is the height above the surface. The effects of buoyancy on the turbulence are characterized by the value of B. This is true for an explicit eddy diffusivity, such as that used in the ECMWF forecast model (Louis et al. 1981), or for a higher-order closure model, such as that of Manton (1983). We therefore parameterize the effects of cumulus cloud by estimating the variation of B with cloud cover γ.

It is found from the thermodynamic equations that, when the air is saturated (i.e. γ=1), the value of B in (2.1) must be replaced by (Manton, 1980)

$$B = g\left\{1-\alpha_1\alpha_3)\frac{1}{\theta}\frac{\partial\theta}{\partial z} + (R_v/R_a - 1 + \alpha_1)\frac{\partial q}{\partial z}\right\} , \tag{2.2}$$

where $\alpha_1 = (L/C_{pa}T - R_v/R_a)/(1 + \alpha_3 L/C_{pa}T)$,

$\alpha_3 = T\frac{\partial s}{\partial T}$,

$T = \theta(p/p_*)^{\kappa} + Lq_c/C_{pa}$, with $\kappa = R_a/C_{pa}$

$q_c = \max(0, q-s)$;

L is the latent heat of vaporization, C_{pa} is the specific heat at constant pressure for dry air, s is the saturation mass fraction for water vapour, T is temperature, q_c is the mass fraction of cloud water, p is the air pressure

and p_* is a reference pressure. Equation (2.2) is derived by retaining only terms of the first order in the mass fraction of water, and it does not account for precipitation which moves relative to the air parcel.

The value of B given by (2.1) is valid for $\gamma=0$ while (2.2) is valid when $\gamma=1$. To account for fractional cloud cover we assumed that an appropriate representation of B is found from a linear combination of (2.1) and (2.2); that is, we take

$$B = \gamma\tilde{B} + (1-\gamma)\tilde{\tilde{B}} , \tag{2.3}$$

where $\tilde{B}$ is given by (2.2) and $\tilde{\tilde{B}}$ is from (2.1). It is readily seen from (2.1) - (2.3) that in general B can be approximated by

$$B = g\{\frac{1}{\theta}\frac{\partial\theta}{\partial z} + (R_v/R_a-1)\frac{\partial q}{\partial z}\} + \alpha_1 g\,\gamma\{\frac{\partial q}{\partial z} - \alpha_3(\frac{1}{\theta}\frac{\partial\theta}{\partial z})\} . \tag{2.4}$$

In the stable region above a well mixed layer, $\partial\theta/\partial z$ is positive while $\partial q/\partial z$ is generally negative. Thus (2.4) shows that the essential effect of cloud is to decrease the mean stability of an air column and so to increase the vertical penetration by turbulent mixing. The value of B given by (2.4) is used throughout the turbulence parameterization so as to enhance the eddy diffusivity.

In order to include (2.4) in a turbulence parameterization, the fractional cloud cover γ and the cloud-top height are estimated from the cumulus cloud model described below. At all heights below the cloud top the value of B is then given by (2.4) with the specified value of γ. This implementation implies that the effects of cloud extend from cloud top to the surface. The extension of (2.4) below cloud base may be supported by the argument that cumulus clouds are generated from the surface layers and so their effects should be extended to the whole region of influence.

3. CLOUD BASE AND CLOUD COVER

The present cloud parameterization is based on the bulk model of Manton (1982). Clouds are assumed to grow in patches of air that extend from the well-mixed layer above the surface, as shown in Fig.1. To determine the top of the mixed layer σ_m, we find the lowest grid-point level σ_{m-1} at which the virtual potential temperature is $\Delta\theta$ greater than that at the top of the surface layer θ_{vs} (i.e. at the lowest grid level σ_N). Thus we take

$$\theta_{vm} = \theta_v(\sigma_m) \tag{3.1}$$

where $\theta_v(\sigma_{m-1}) > \theta_{vs} + \Delta\theta$.

(The vertical coordinate is assumed to be the normalized pressure $\sigma = p/p_s$, where p_s is the surface pressure. The grid levels are at $\sigma = \sigma_k$, k=1,2,..,N).

The deformation of the top of the mixed layer is caused by thermals that rise from the surface and are consequently driven by the surface buoyancy flux $\overline{b'w'_s}$

$$\overline{b'w'_s} = g\{\overline{\theta'w'_s}/\theta_s/\theta_s + (R_v/R_a - 1)\,\overline{q'w'_s}\} \tag{3.2}$$

where $\overline{\theta'w'_s}$ and $\overline{q'w'_s}$ are the surface fluxes of potential temperature and moisture. The flux $\overline{b'w'_s}$ is found from the turbulence parameterization of the surface layer. The velocity scale w_* for thermals in the well-mixed layer is given by

$$w_* = (\overline{b'w'_s}\ H_m)^{1/3}\ , \tag{3.3}$$

where H_m is the height of the mixed layer. The geometric height H_m is found by integrating the hydrostatic pressure equation from the surface to σ_m.

In the absence of condensation the top of the mixed-layer patches would extend to the level σ_p, which is dependent upon the penetration of thermals into the stable air above the mixed layer. Manton (1982) deduces a prognostic equation for σ_p. In the present work the distance $\sigma_m - \sigma_p$ is assumed to be algebraically related to the distance that individual thermals can penetrate into the overlying air, so that σ_p is simply a diagnosed variable. The momentum balance for a thermal penetrating a stable region is estimated by the equation

$$\frac{d}{dz}\left(\frac{1}{2}w^2\right) = -\frac{\Delta\rho}{\rho}g \quad , \tag{3.4}$$

where w is the thermal velocity and $\Delta\rho$ is the density difference between the thermal and its environment. Using the initial condition

$$w = c_1 w_* \text{ at } \sigma = \sigma_m \tag{3.5}$$

where c_1 is a constant, we integrate (3.4) to the level σ_p at which w=0. In particular, the change in w between the grid-point levels k+1 and k is given by

$$w_k^2 = w_{k+1}^2 - 2R_a(\theta_{v,k} - \theta_{vm})\,\sigma_{k+\frac{1}{2}}^{\kappa-1}\,\Delta\sigma_{k+\frac{1}{2}} \; ;$$

If $w_k^2 < 0$ then the penetration distance is found to be

$$\sigma_p = \sigma_{k+1} - w_{k+1}^2/2\,R_a(\theta_{v,k} - \theta_{vm})\,\sigma_{k+\frac{1}{2}}^{\kappa-1} \quad , \tag{3.6}$$

where $w_{k+1}^2 = c_1^2 w_*^2 - \sum_{i=m-1}^{k+2} 2\,R_a(\theta_{v,i} - \theta_{vm})\sigma_{i+\frac{1}{2}}^{\kappa-1}\,\Delta\sigma_{i+\frac{1}{2}}$

Equations (3.5) - (3.6) specify the depth of patches of mixed-layer air in the absence of condensation. If the condensation lifting level of mixed-layer is higher than σ_p then clearly there is no cumulus cloud. On the other hand as the condensation level falls, the fractional cloud cover γ should monotonically increase as more of each mixed-layer patch becomes saturated. If the condensation level is less than or equal to the mixed-layer height then

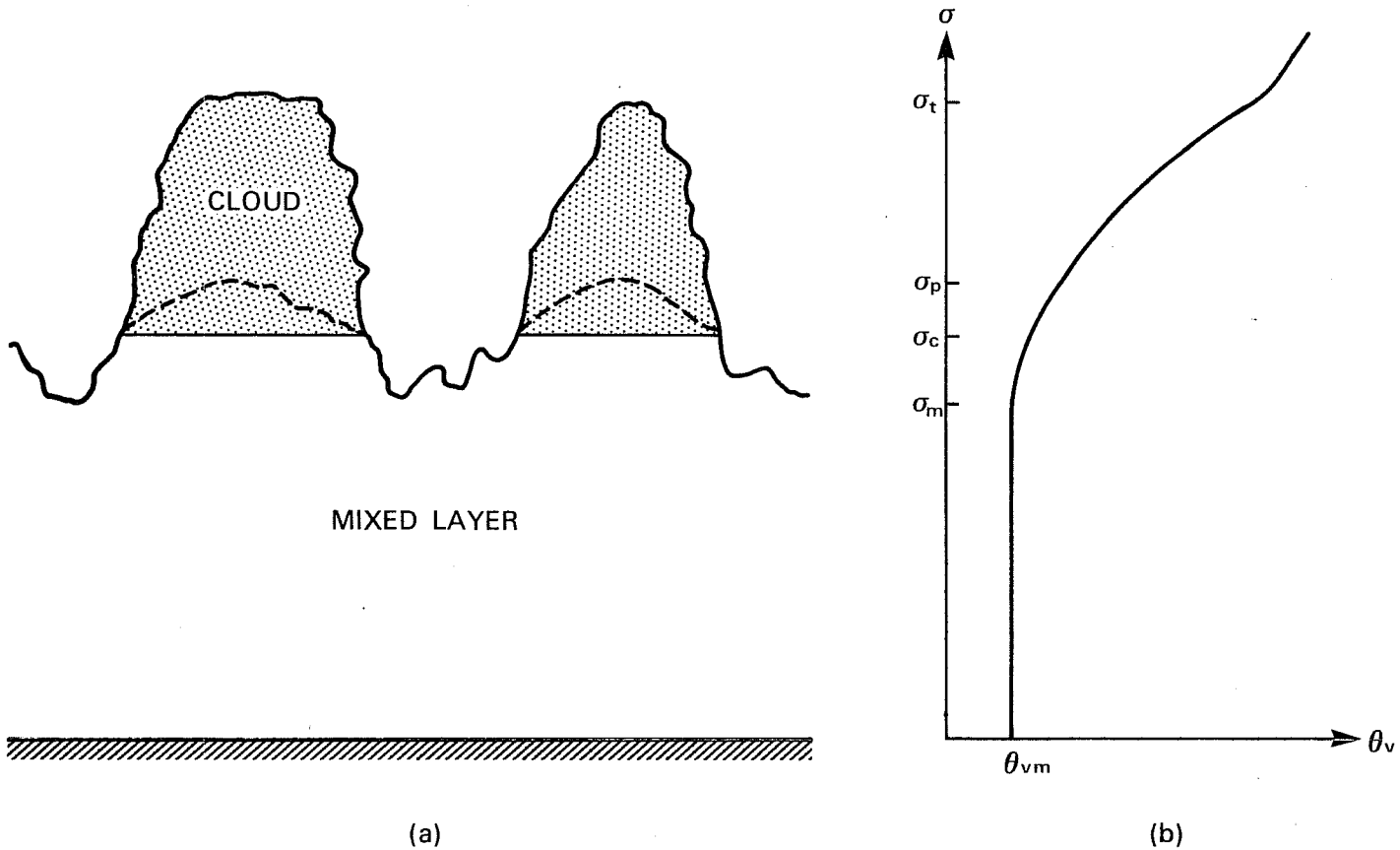

Fig. 1. (a) Structure of model boundary layer with shallow cumulus convection. Mixed-layer patches extend beyond the tops of the mixed layer H_m (b) Shape of visual potential temperature profile $\theta_v(\sigma)$ for the model boundary layer.

the cloud cover is unity and a stratocumulus deck is formed. We assume that this variation of cloud cover with condensation level can be approximated by

$$\gamma = \min\{1, \max[0, (\sigma_c - \sigma_p)/(\sigma_m - \sigma_p)]\}^{c_2}, \qquad (3.7)$$

where σ_c is the condensation lifting level for mixed-layer air and c_2 is a constant. The results of Manton (1982) suggest that c_2 should be greater than unity so that γ is small unless cloud base is near the top of the mixed layer.

To calculate the condensation level σ_c we assume that the air in thermals is represented by the mean air properties at the top of the mixed layer, where the potential temperature is θ_m and the mass fraction of water is q_m. Thus the temperature T in a rising thermal at level σ is given by

$$T = \theta_m \sigma^{\kappa} .$$

Condensation occurs when q_m equals the local saturation mass fraction of water, and so we have from (2.2)

$$q_m = s_m (\sigma_m/\sigma_c) - \alpha_{3,m} \{1 - (\sigma_c/\sigma_m)^{\kappa}\}, \qquad (3.8)$$

where s_m is the saturation mass fraction at σ_m. The first term on the right-hand side of (3.8) accounts for the pressure difference between σ_m and σ_c while the second term accounts for the temperature change in s. The condensation level is therefore approximated by

$$\delta_c = (s_m - q_m)/(\alpha_{3,m} \kappa - s_m), \qquad (3.9)$$

where $\sigma_c = \sigma_m (1-\delta_c)$.

4. CLOUD TOP

The depth of penetration of shallow cumulus clouds can be estimated by the simple Lagrangian parcel model in which a cloud parcel entrains the mean environmental air as it rises. We therefore assume that the liquid-water potential temperature $\tilde{\theta}$ and the water mass fraction $\tilde{q}$ in cloud may be found from the equations

$$\frac{d\tilde{\theta}}{d\sigma} = \lambda(\tilde{\theta} - \theta) \quad \text{and} \quad \frac{d\tilde{q}}{d\sigma} = \lambda(\tilde{q} - q) \ , \tag{4.1}$$

where λ is an entrainment constant. These equations can be integrated between grid levels σ_{k+1} and σ_k to yield

$$\begin{aligned} \tilde{\theta}_k &= \theta_{k+\frac{1}{2}} + (\tilde{\theta}_{k+1} - \theta_{k+\frac{1}{2}}) \exp\{\lambda(\sigma_k - \sigma_{k+1})\} \ , \\ \tilde{q}_k &= q_{k+\frac{1}{2}} + (\tilde{q}_{k+1} - q_{k+\frac{1}{2}}) \exp\{\lambda(\sigma_k - \sigma_{k+1})\} \ . \end{aligned} \tag{4.2}$$

The initial conditions for (4.2) are

$$\tilde{\theta} = \theta_m \text{ and } \tilde{q} = s \text{ at } \sigma = \sigma_c .$$

Equations (4.2) are integrated up to the level at which the cloud parcel becomes neutrally buoyant. It is therefore necessary to determine the temperture $\tilde{T}_k$ in the cloud at each level.

As in (3.8), the change in saturation mass fraction of water $\tilde{s}$ between levels k+1 and k is approximated by

$$\tilde{s}_k = \tilde{s}_{k+1}(\sigma_{k+1}/\sigma_k) + \alpha_{3,k+1}(\tilde{T}_k/\tilde{T}_{k+1} - 1) \tag{4.3}$$

It is also seen from (2.2) that

$$\tilde{T}_k = \tilde{\theta}_k \, \sigma_k^{\kappa} + (L/C_{pa})(\tilde{q}_k - \tilde{s}_k) \tag{4.4}$$

Putting (4.3) into (4.4) we find that the cloud temperature $\tilde{T}_k$ is given by the equation

$$\tilde{T}_k\{1 + \alpha_{3,k+1}(L/C_{pa}\tilde{T}_{k+1})\} = \tilde{\theta}_k\, \sigma_k^{\kappa} + (L/C_{pa})\{\tilde{q}_k - \tilde{s}_{k+1}(\sigma_{k+1}/\sigma_k) + \alpha_{3,k+1}\} \qquad (4.5)$$

With $\tilde{T}_k$ and σ_k specified, the saturation mass fraction $\tilde{s}_k$ can be found at level k in the cloud.

A necessary condition for cloud to exist is that $\tilde{q} \geq \tilde{s}$.

The main test for cloud top is the comparison of the density in cloud $\tilde{\rho}_k$ with the mean environment density ρ . The equations of state in the clear and cloudy air are

$$p_k/\rho_k\, R_a = T_k\{1 + (R_v/R_a - 1)q_k\},$$

$$p_k/\tilde{\rho}_k\, R_a = \tilde{T}_k\{1 + (R_v/R_a - 1)\tilde{q}_k - (R_v/R_a)(\tilde{q}_k - \tilde{s}_k)\}.$$

Cloud top σ_t is defined as the first level k where

$$p_k/\rho_k\, R_a \geq p_k/\tilde{\rho}\, R_a \qquad (4.6)$$

The cloud scheme described in Sects. 2,3 and 4 models the enhanced mixing due to shallow cumulus cloud.

5. CUMULUS PRECIPITATION

The development of precipitation in shallow cumulus has two effects. First it leads to local heating and drying of the atmosphere as the precipitation falls from a given cloud level. However, evaporation of the precipitation into the environment produces cooling and moistening in both the cloud layer and below cloud base. The present parameterization of precipitation essentially follows Kessler (1969).

The cloud model in Sect.4 predicts the total water $\tilde{q}_k$ and saturation mass fraction $\tilde{s}_k$ at level k in a shallow cumulus cloud. We assume that the liquid water $\tilde{q}_k - \tilde{s}_k$ produces an increment in the total precipitation $\Delta q_{r,k}$ falling through the level k, such that

$$\Delta q_{r,k} = \max\{0,\ c_3(\tilde{q}_k - \tilde{s}_k - q_{cr})\}\ , \tag{5.1}$$

where c_3 is a constant and q_{cr} is a (constant) threshold water mass fraction that must be exceeded before precipitation occurs. Kessler (1969) shows that a precipitation mass fraction q_r corresponds to a rainfall flux R, where

$$R = a_1\ (\rho\ q_r)^{1.125}, \tag{5.2}$$

ρ is the air density and $a_1 = 5.09$ gm m^{-2} s^{-1} (gm m^{-3})$^{-1.125}$. We use (5.2) to estimate the increment to the net rainfall flux ΔR_k at level k due to the increment in rainwater $\Delta q_{r,k}$, such that

$$\Delta R_k = a_1\ (p_s\ \sigma_k\ \Delta q_{r,k}/R_a\ \tilde{T}_k)^{1.125}, \tag{5.3}$$

where $a_1 = 12.08$ kg m^{-2} s^{-1} (kg m^{-3})$^{-1.125}$ and p_s is the surface pressure.

The rate of evaporation of precipitation E into a subsaturated environment is found by Kessler (1969) to be

$$E = a_2\ \rho\ (s-q)(\rho q_r)^{0.65}\ , \tag{5.4}$$

where $a_2 = 5.44 \times 10^{-4}$ gm m^{-3} s^{-1} (gm m^{-3})$^{-1.65}$. Using (5.2), (5.4) and the hydrostatic pressure equation we see that if R_k is the net rainfall flux at level k then evaporation produces a decrement ΔE_k in the rainfall flux such that for $s_k > q_k$

$$\Delta E_k = a_2 (p_s \, \Delta\sigma_k / g)(s_k - q_k)(R_k / a_1)^{0.5778}, \tag{5.5}$$

where $a_2 = 4.85 \times 10^{-2}$ kg m^{-3} s^{-1} (kg m^{-3})$^{-1.65}$. The net rainfall flux is given by

$$R_k = \sum_{i=1}^{k-1} (\Delta R_i - \Delta E_i), \tag{5.6}$$

with $R_1 = 0$.

Equations (5.1), (5.3), (5.5) and (5.6) describe the development of the net precipitation flux due to shallow cumulus convection. The net cumulus precipitation flux to the surface P_{cu} is seen from (5.6) to be

$$P_{cu} = \gamma \sum_{k=1}^{N} (\Delta R_k - \Delta E_k) , \tag{5.7}$$

where γ accounts for the fractional cloud cover. The increment in rainfall flux at level k in the atmosphere yields a net loss of water mass fraction δq_{cu} over a time step $2\Delta t$, where

$$\delta q_{cu,k} = 2\Delta t \; \gamma \; (\Delta R_k - \Delta E_k) \; g / (p_s \, \Delta\sigma_k) . \tag{5.8}$$

The corresponding increase in latent heat produces the temperature increment δT_{cu}, where

$$\delta T_{cu,k} = (L / C_{pa}) \; \delta q_{cu,k} . \tag{5.9}$$

6. UNDISTURBED BOMEX PERIOD

Holland and Rasmusson (1973) produce energy budgets for the detailed observations obtained over a 5-day period (22-26 June, 1969) during the Barbados Oceanographic and Meteorological Experiment (BOMEX). The results represent an undisturbed tropical situation (latitude 15°N) in which the vertical flux from trade-wind cumulus clouds balances large-scale subsidence in the atmosphere below about 700 mb. The case is therefore suitable for testing the behaviour of parameterizations of shallow convection.

Most of the results described below are carried out using the one-dimensional model of Manton (1983) with a time-step Δt of 900s and 15 vertical grid-point levels (N=15). The initial conditions and the external forcing terms in the equations of motion were derived by M. Tiedtke (personal communication) and they are shown in Table 1. The velocity profile is kept fixed while the temperature T and moisture q profiles are integrated over three days. The surface conditions correspond to a tropical ocean with p_s = 1015 mb and T_s = 301.64 K.

We first consider the results of the one-dimensional model when there is no cloud parameterization. Fig.2 compares the initial sounding with the profiles of potential temperature θ and water mass fraction q at time t = 72 hr when turbulent mixing is represented by the ECMWF eddy diffusivity (Louis et al. 1981). The air column is clearly not in equilibrium during the integration period. The effects of turbulence are restricted to a saturated mixed layer below 900 mb. Thus an increasingly strong inversion forms owing to the large-scale heating and drying above 900 mb. The maximum in the large-scale heating rate at 850 mb causes a dry-adiabatic mixed layer to form between 850 and

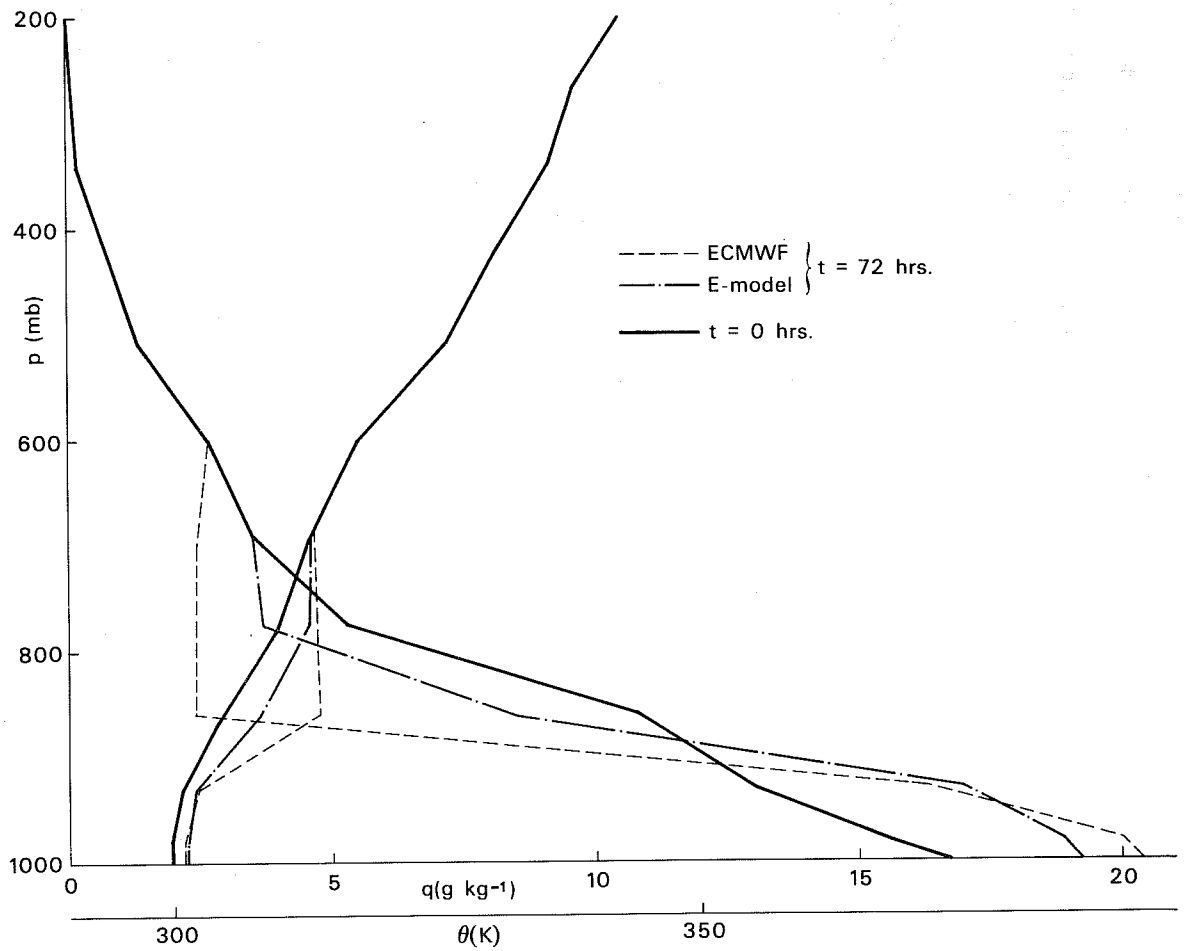

Fig. 2. Profiles of potential temperature Θ and water mass fraction q for the BOMEX undisturbed conditions with different turbulence parameterizations in the integration but no cumulus cloud parameterizations ; Δt=900s and N=15.

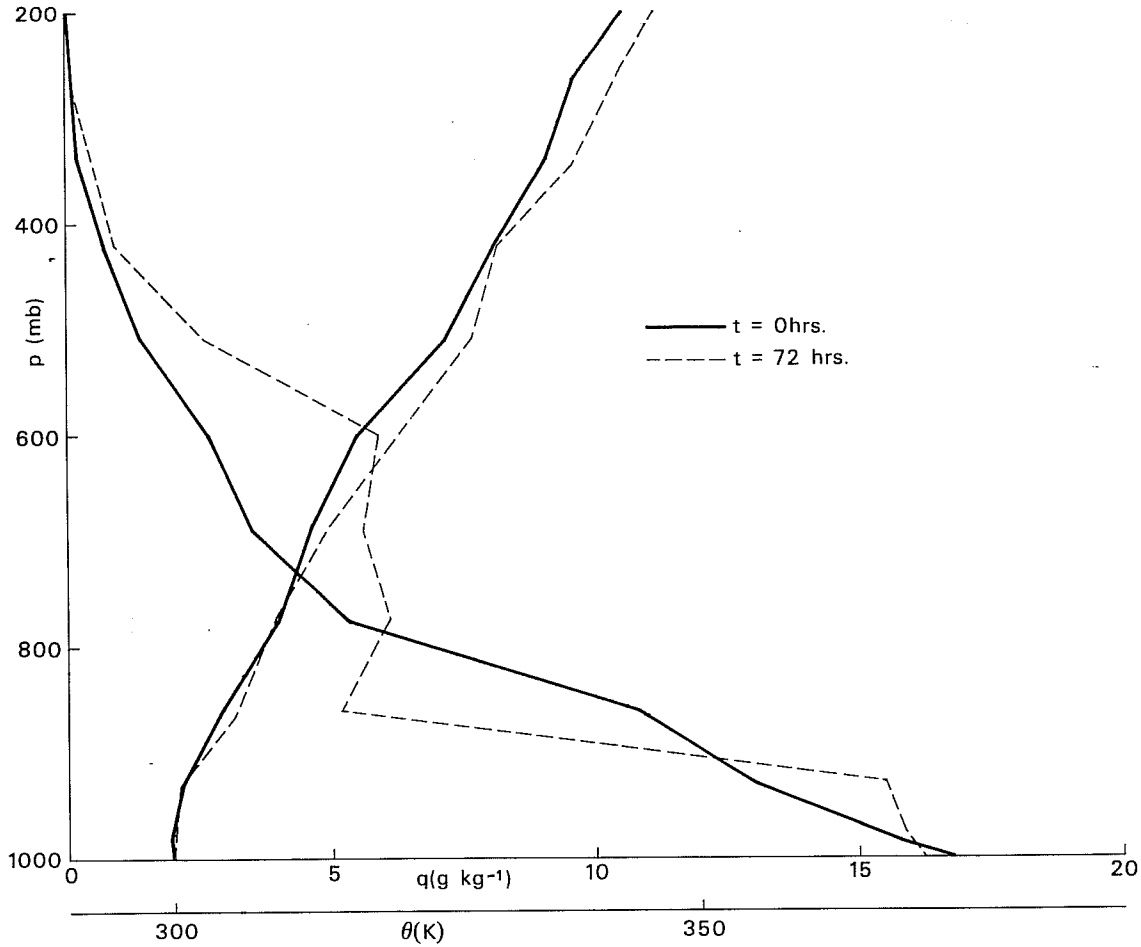

Fig. 3. Profiles of potential temperature θ and water mass fraction q for the BOMEX undisturbed conditions with the ECMWF turbulence scheme and the Arakawa-Schubert cumulus parameterization ; Δt=900s and N=15.

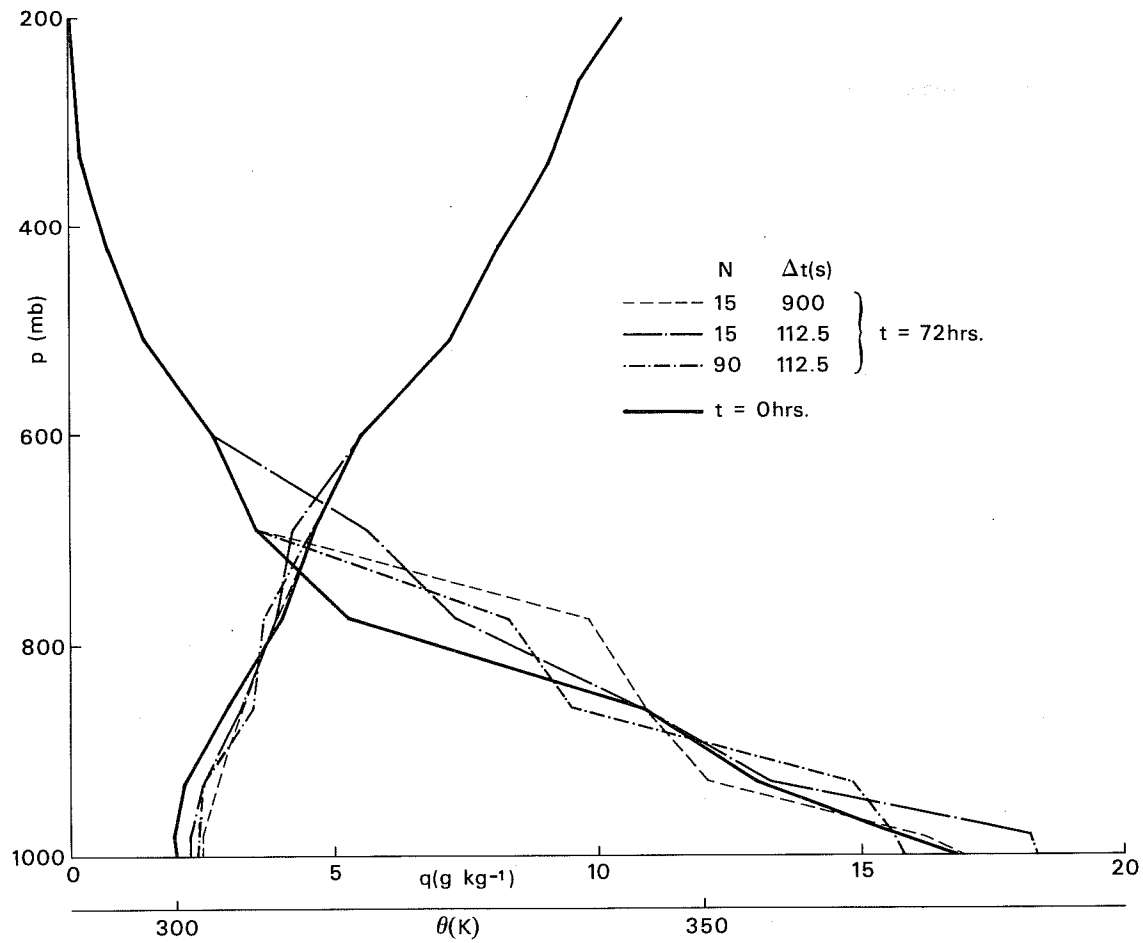

Fig. 4. Profiles of potential temperature θ and water mass fraction q for the BOMEX undisturbed conditions with the ECMWF turbulence scheme and the present shallow-cumulus scheme.

700 mb after about 54 hours. The absence of cumulus convection causes the average surface flux of latent heat to be only 120 W m^{-2}, compared with the observed flux of 175 W m^{-2}. Consequently the total latent heat content of the air column drops from 99 to 85 MJ m^{-2} over the 72-hour integration period. If the integration is carried out with the ECMWF forecast model, which includes the Kuo (1974) parameterization for cumulus cloud, then the results are essentially unchanged because cumulus convection is suppressed by the inversion.

Fig.2 also shows the final profiles of θ and q when the ECMWF scheme for turbulent diffusion is replaced by the turbulent-energy scheme (E-model) of Manton (1983). Earlier tests show that the E-model induces greater vertical diffusion than the ECMWF scheme and this feature is evident in the present results where the enhanced turbulence below 900 mb allows some of the effects of subsidence to be balanced above the inversion. However, it is apparent that there is an excess of moisture below and a deficit above 900 mb, owing to the lack of a cumulus parameterization scheme.

Tiedtke (1981) decribes experiments with the ECMWF forecast model in which the Kuo convection scheme is replaced by the Arakawa-Schubert (1974) parameterization. Fig.3 indicates that the Arakawa-Schubert scheme does give rise to the transport of moisture across the inversion. This is reflected in the latent heat flux at the surface, which is somewhat overestimated with an average value of 210 W m^{-2}. The cumulus convection is seen however to penetrate too deeply and it produces significant changes at 200 mb. Moreover the moisture transport is not represented well and a deep region of uniform q is developed so that q is underestimated at 850 mb and overestimated at 600 mb. The Arakawa-Schubert scheme would therefore appear to be too responsive when it transports moisture from the top of the boundary layer into the middle troposphere in suppressed conditions.

In order to use the present shallow convection scheme, six constants must be specified: $\Delta\theta$ in (3.1), c_1 in (3.5), c_2 in (3.7), λ in (4.1), and c_3 and q_{cr} in (5.1). Precipitation-sized particles are generally not found in a cumulus cloud until the liquid-water mass fraction is more than about 1 g kg^{-1} and so we take the threshold liquid-water constant q_{cr} to be 2 g kg^{-1} to provide a conservative estimate for the onset of widspread rain. Negligible surface precipitation was observed during the undisturbed BOMEX period and this condition is satisfied by setting the rain-fraction constant c_3 equal to 01. The temperature increment $\Delta\theta$ defines the top of the mixed layer and hence the air parcel which is lifted to determine cloud base. It is found that $\Delta\theta$ must be rather large so that the estimated cloud base does not fluctuate greatly. We therefore take $\Delta\theta$=1K. The presence or absence of cloud is controlled by the penetration constant c_1. By setting c_1=20 we find that cumulus convection can provide a reasonably steady forcing. Entrainment is required to limit the penetration of buoyant cloud parcels and steady estimates for cloud top are obtained when the entrainment constant λ is equal to 8. The net flux induced by cumulus convection is determined primarily by the cloud-cover constan c_2. As the convection scheme tends to overestimate the moisture flux we find that c_2 needs to be quite large. Appropriate fluxes are obtained with c_2=4.

Fig.4 shows the profiles of θ and q obtained when the ECMWF diffusion scheme is combined with the present cumulus convection scheme. Comparing Figs.2 and 4 for the standard resolution case of N=15 and Δt=900s we see that the convection scheme adequately compensates for the large-scale subsidence. Although the air below is slightly warmed, the temperature profile is relatively steady when cumulus convection is included. The humidity below

900 mb is reduced by the transfer of moisture to the region between 700 mb and 900 mb. This vertical transport is slightly excessive so that the average surface flux of latent heat is 189 W m^{-2} and the total latent heat content of the air column increases from 99 to 107 MJ m^{-2} over the 72-hour integration period.

In addition to the standard resolution case, Fig.4 gives profiles of θ and q when the temporal and spatial resolution are increase. Although the gross properties of the profiles are maintained it is clear that the detailed behaviour of θ and q is sensitive to truncation error. This sensitivity is most evident from Fig.5, which shows the variation of cloud cover γ with time for the different resolutions. The sensitivity arises because γ varies with the fourth power of the difference between the penetration distance and the condensation level for thermals, as given by (3.7). While the average cloud cover is consistent among the cases, the temporal variation is great. A particular feature is that the cumulus activity tends to be intermittent, producing large corrections rather than small continuous adjustments.

Fig.6 displays the potential temperature and water mass fraction profiles when the present cumulus scheme is used with the E-model for turbulent diffusion. Comparison with Fig.4 shows that the convection reduces the humidity below 900 mb by transporting moisture up to 700 mb. Owing to the greater diffusion of the E-model, the vertical transport is somewhat excessive and the average surface flux of latent heat is 120 W m^{-2} for the standard resolution case. As with the ECMWF diffusion, the solution is found to be sensitive to the spatial and temporal resolution. However, Fig.7 shows that the temporal variation of cloud cover with E-diffusion is more consistent with the ECMWF diffusion.

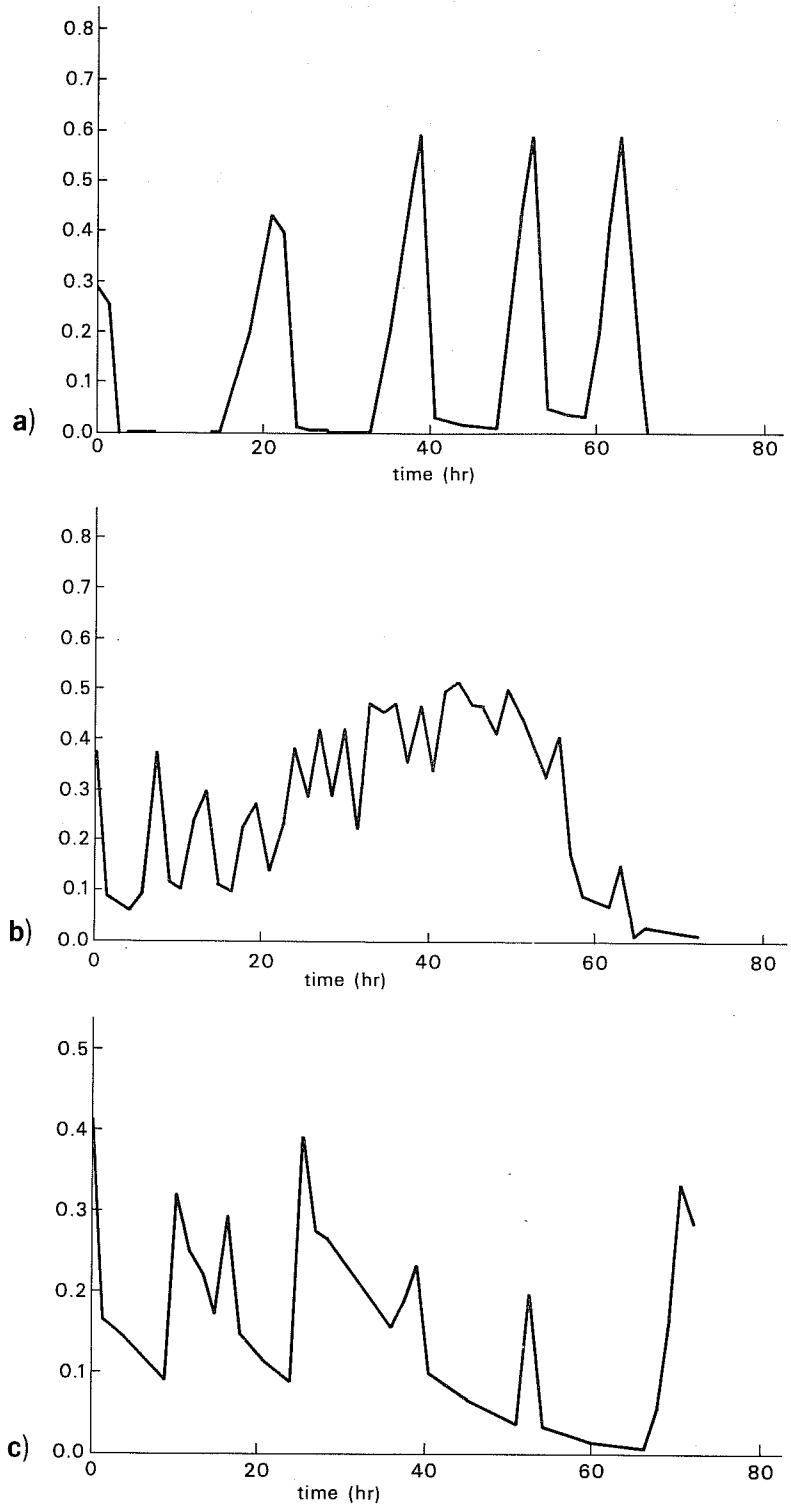

Fig. 5. Variation of fractional cloud cover with time for the BOMEX undisturbed conditions with the ECMWF turbulence scheme and the present shallow-cumulus scheme ; (a) N=15, Δt=900s ; (b) N=15, Δt=112.5s ; (c) N=90, Δt=112.5s.

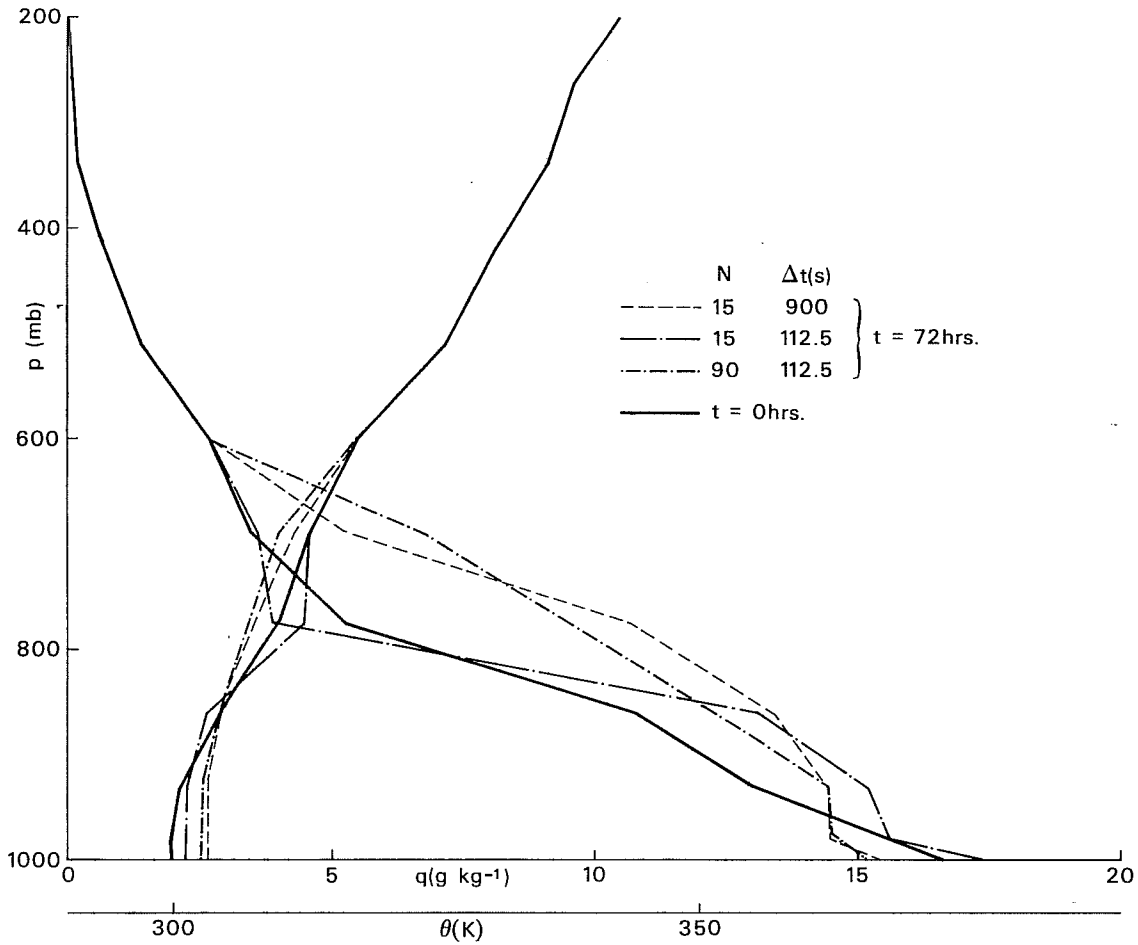

Fig. 6. Profiles of potential temperature Θ and water mass fraction q for the BOMEX undisturbed conditions with the E-model turbulence scheme and the present shallow-cumulus scheme.

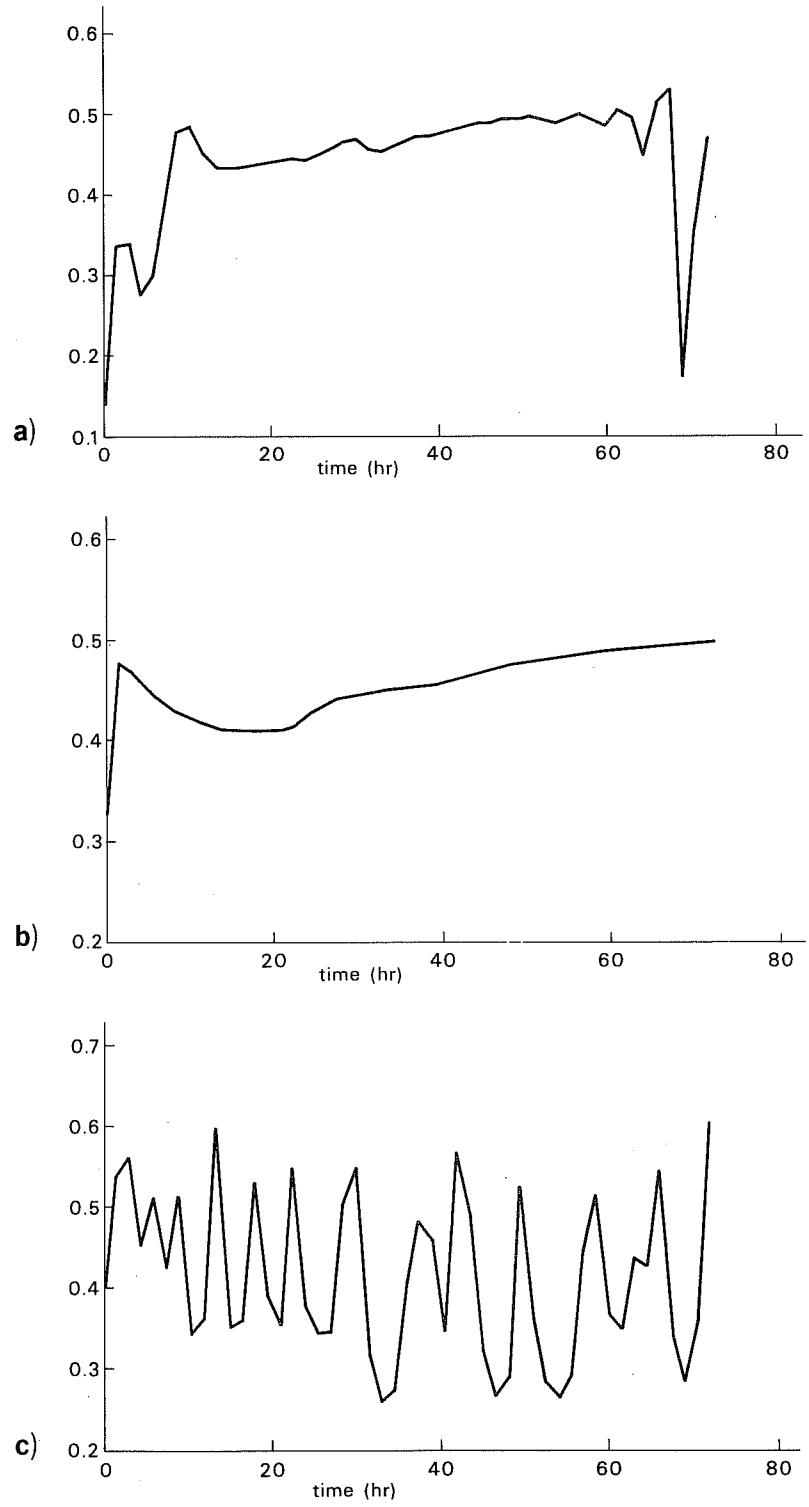

Fig. 7. Variation of fractional cloud cover with time for the BOMEX undisturbed conditions with the E-model turbulence scheme and the present shallow-cumulus scheme ; (a)N=15, Δt=900s ; (b)N=15, Δt=112.5s ; (c)N=90, Δt=112.5s.

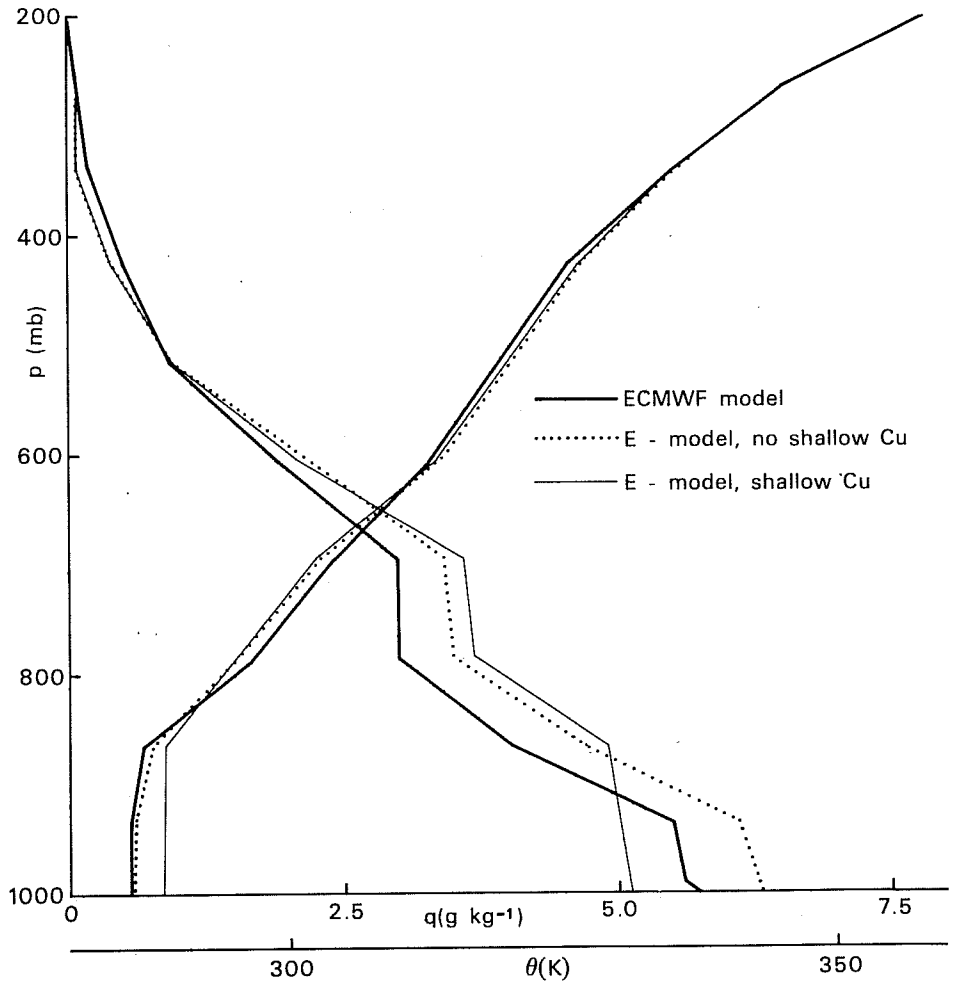

Fig. 8. Profiles of potential temperature Θ and water mass fraction q at 28° N, 129° E after 24 hrs of integration of the ECMWF forecast model, starting with the FGGE analysis of 18/1/79.

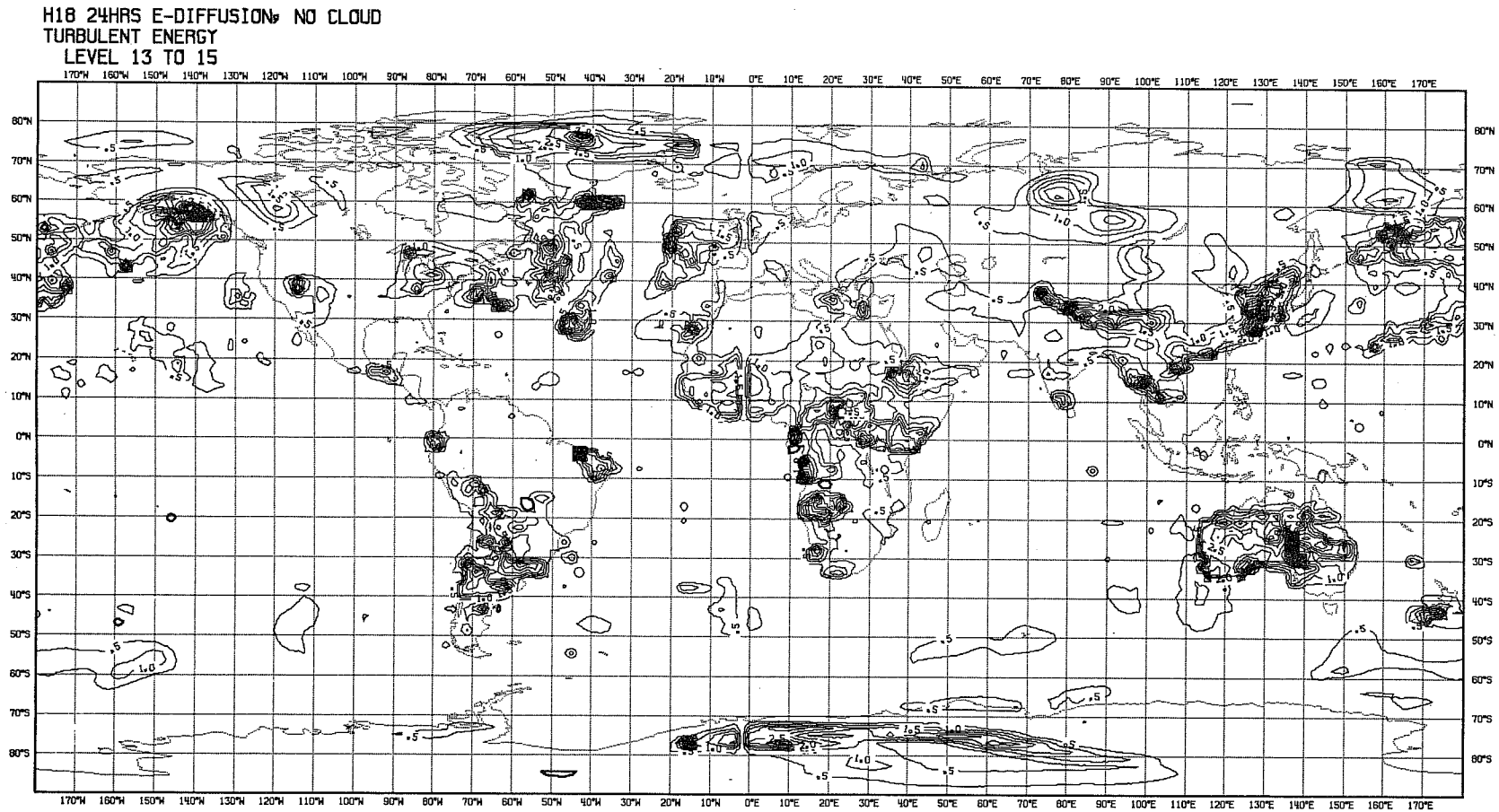

Fig. 9. Global distribution of the average turbulence level in the boundary layer (below about 900 mb) after 24 hrs. of integration of the ECMWF forecast model, starting with the FGGE analysis of 18/1/79 ; (a) E-model turbulence without shallow convection.

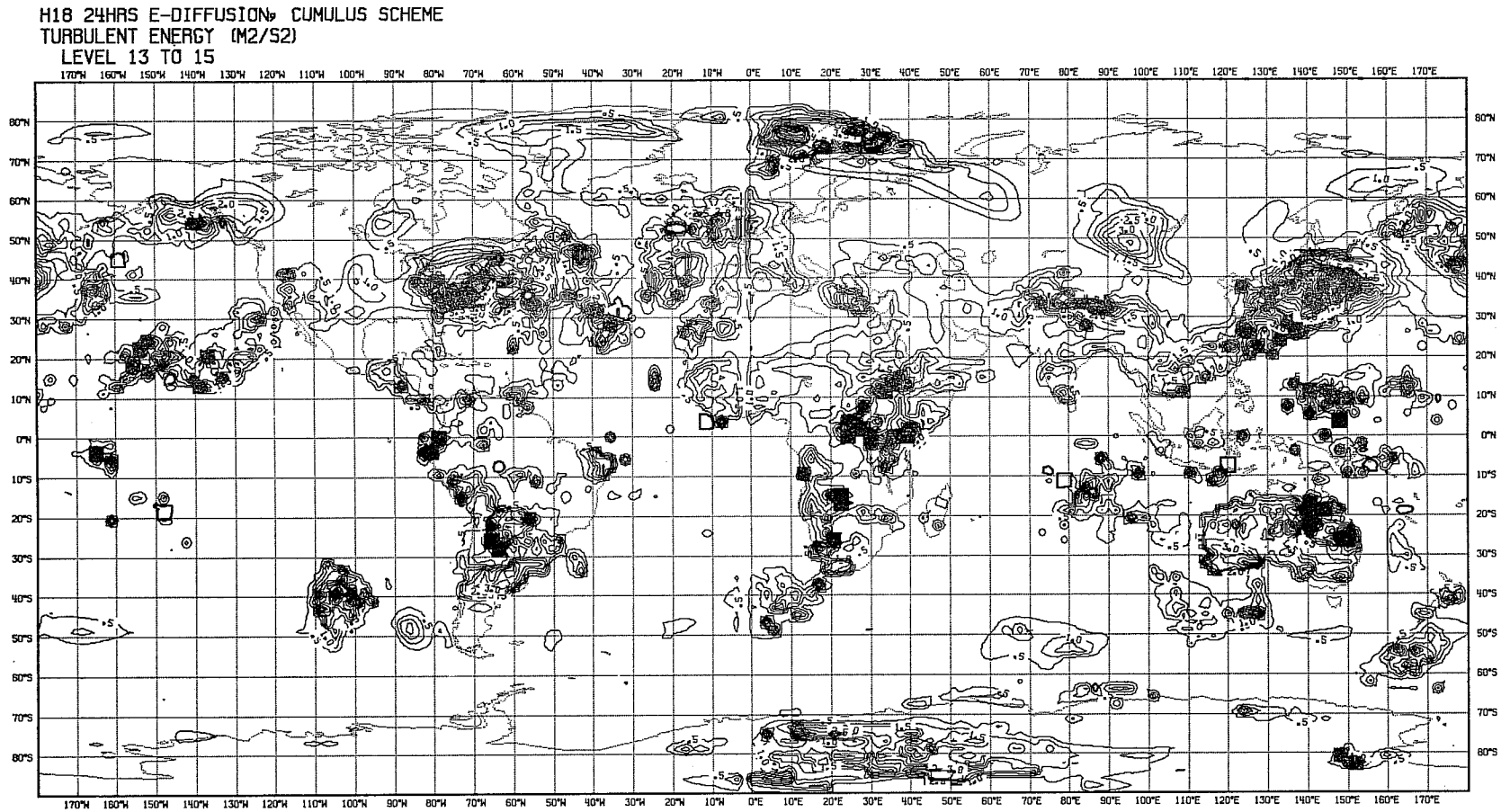

Fig. 9 (b) E-model turbulence with shallow convection.

7. COLD-AIR OUTBREAK

Tiedtke (1981) describes a case study of a polar outbreak over the West Pacific during the FGGE observing period (18/1/79) in which the ECMWF forecast model is integrated for one day and the development of a moist mixed layer over the sea is studied. That case has been repeated with the E-model for turbulent mixing and the present cumulus convection scheme in the forecast model. Fig.8 shows the profiles of potential temperature θ and water mass fraction q at the location 28°N, 129°E after 24 hours of integration. In the absence of shallow convection, moisture is trapped below about 930 mb although the gradient of θ between 930 and 860 mb is rather weak. However, the enhanced mixing of the E-model allows more moisture to be transported up to 700 mb. The vertical transfer of moisture from the mixed layer into the stable region below 700 mb is greatly increased when the present shallow convection scheme is included. Thus the mixed layer extends to 850 mb and the relative humidity at 700 mb is increased to about 80%.

The effect of shallow convection on mixing in the boundary layer is also illustrated in Fig.9 which shows the global distribution of turbulent energy after 24 hours of integration. It is clear that the turbulence level is generally increased in the boundary layer when the convection scheme is included. In the region of the North-West Pacific where the cold-air outbreak occurs, both the extent and intensity of the boundary-layer turbulence is increased. In other areas the convection scheme causes the turbulence level to be enhanced from less than 1 to several $m^2\ s^{-2}$; for example, in a high-pressure region in the North Pacific near 20°N and a low-presure area in the South Pacific near 50°S.

8. CONCLUSIONS

Tests with the ECMWF forecast model suggest that the Kuo (1974) and the Arakawa-Scubert (1974) convection schemes do not accurately represent the vertical transport due to shallow cumulus clouds in undisturbed tropical conditions. The present cumuls scheme is developed under the assumption that shallow convection tends simply to enhance turbulent mixing in the stable region directly above the well-mixed layer near the surface. Thus cloud reduces the effective stability of the region and the eddy diffusivity is increased. The scheme allows both the momentum and thermodynamic fields to be adjusted. The convection scheme is applied with both the ECMWF turbulence parameterization and the higher-order closure model of Manton (1983).

The convection scheme is found to be particularly effective in enhancing the vertical transfer of moisture when turbulent mixing is represented by the ECMWF scheme. For the case of the BOMEX undisturbed period (Holland and Rusmusson, 1973), the convection is found to compensate adequately for drying and warming effects of subsidence above the well-mixed layer. The convection is found to occur intermittently in time so that the atmospheric variables generally do not change smoothly and the detailed results are sensitive to the spatial and temporal resolution of the numerical integration.

Earlier tests (Manton 1983) indicate that the higher-order closure scheme for turbulence (E-model) yields more vertical mixing than the ECMWF model. The effects of the shallow convection scheme are therefore not expected to be as marked when used with the E-model. However, the convection is still found to reduce the humidity in the mixed layer and to moisten the stable region below 700 mb for the BOMEX undisturbed case study. This feature is particularly noticeable in a global integration starting with the FGGE analysis of 18/1/79, where there is a polar outbreak over the North-West Pacific.

The global integration shows that the shallow convection scheme produces enhanced boundary-layer turbulence in both disturbed and undisturbed regions over the ocean.

Although the convection scheme may be used to predict the fractional cloud cover of shallow cumulus (independently of any turbulent effects), this feature has not been tested in the present work.

Table 1 Initial conditions and forcing terms for BOMEX undisturbed period.

p (mb)	u (m s^{-1})	v (m s^{-1})	T (K)	q (g kg^{-1})	$\dot{T}_a$ (K dy^{-1})	$\dot{q}_a$ (g kg^{-1} dy^{-1})
25	-1.5	-1.0	231.9	0.7	0.	0.
78	-1.5	-1.0	202.1	0.001	0.	0.
134	-1.5	-1.0	197.1	0.001	0.	0.
196	-1.5	-1.0	214.0	0.001	0.	0.
264	-1.5	-1.0	230.0	0.1	0.	0.
339	-1.5	-1.0	245.1	0.2	0.	0.
420	-1.5	-1.0	256.9	0.7	0.	0.
508	-1.5	-1.0	267.3	1.4	0.	0.
598	-2.7	-0.7	272.8	2.7	0.	0.
688	-5.0	0.5	280.1	3.5	0.	0.
777	-6.7	1.2	287.1	5.3	1.01	-0.7
858	-8.7	0.6	290.2	10.8	3.26	-3.5
928	-8.8	0.2	293.1	13.0	-2.71	-1.4
981	-8.7	0.0	296.8	16.5	-2.64	-0.9
1011	-7.2	-0.4	299.8	17.4	-2.61	-0.7

REFERENCES

Arakawa, A. and Schubert, W.H. 1974: Interaction of a cumulus cloud ensemble with the large-scale environment, Part I. J.Atmos.Sci., 31, 674-701.

Kessler, E. 1969: On the distribution and continuity of water substance in atmospheric circulations. AMS.Met.Mon., 10, No.32, 84 pp.

Kuo, H.L. 1974: Further studies of the parameterization of the influence of cumulus convection on large-scale flow. J.Atmos.Sci., 31, 1232-1240.

Louis, J.-F., Tiedtke, M. and Geleyn, J.-F. 1981: A short history of the PBL parameterization at ECMWF. ECMWF Workshop on Planetary Boundary Layer Parameterization, 25-27 November 1981, Reading, England, 59-80 pp.

Manton, M.J. 1980: On the modelling of mixed layers and entrainment in cumulus cloud. Boundary-Layer Met, 19, 337-358.

Manton, M.J. 1982: A model of fair-weather cumulus convection. Boundary-Layer Met, 22, 91-107.

Manton, M.J. 1983: On the parameterisation of vertical diffusion in large-scale atmospheric models. ECMWF Tech.Rep.No.39, pp.36.

Tiedtke, M. 1981: Assessment of the PBL flow in the EC-model. ECMWF Workshop on Planetary Boundary Layer Parameterization, 25-27 November 1981, Reading, England, 155-192 pp.